Ecological Indicators 157 (2023) 111252

Contents lists available at ScienceDirect

Ecological Indicators

journal homepage: www.elsevier.com/locate/ecolind

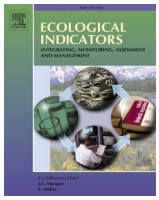

Climate change impacts on streamflow, sediment load and carbon fluxes in the Lena River delta

Sergey Chalov [a,b,c,*], Kristina Prokopeva [a], Dmitry Magritsky [a], Vadim Grigoriev [a], Evgeniya Fingert [a], Michal Habel [c], Bennet Juhls [d], Anne Morgenstern [d], Pier Paul Overduin [d], Nikolay Kasimov [a]

[a] Faculty of Geography, Moscow, Lomonosov Moscow State University, Moscow 119234, Russia
[b] Institute of Ecology and Environment, Kazan Federal University, Kazan 420097, Russia
[c] Faculty of Geographical Sciences, Kazimierz Wielki University, Bydgoszcz 85-064 , Poland
[d] Permafrost Research Section, Alfred Wegener Institute Helmholtz Centre for Polar and Marine Research, Potsdam 14473, Germany

ARTICLE INFO

Keywords:
Climate change
Long-term change
ERA5
Landsat
Lena River Delta
Particulate and dissolved organic carbon
Suspended sediment

ABSTRACT

Water and sediment supply are essential to the health of deltaic ecosystems. Diverse datasets were integrated to better understand how climate change is shifting the supply of water and sediment to the largest polar distributary channel pattern – the Lena River Delta. Here the increase in warming rate from an average air temperature is from 4.1 °C for the period 1950–99 to 6.1 °C during 2000–21, which is higher than in the adjacent polar regions. Streamflow and sediment yield entering the Lena Delta have increased since 1988 by 56.3 km^3 and 6.1×10^6 t, respectively; meanwhile, the Lena River's increases in water temperature in June, July–August and September were found to be as much as 1.1, 0.6 and 0.05 °C. These changes have a pronounced effect on sediment regimes in particular parts of the delta. Based on analyses of correlations between various hydro-climatic drivers and sediment concentration changes across particular distributaries of the Lena Delta extracted from Landsat datasets, bank degradation driven by thermal erosional processes (which are in turn related to air and soil temperature increases) is proved to be the primary factor of the sediment regime in the delta. The study also highlights that sediment load changes are sensitive to wind speed due to remobilization of bottom sediment. Sums of daily air temperature and wind speed over 3 days are correlated with sediment concentration changes in the delta. The results also indicate that carbon transport across the delta (both POC and DOC) depends on sediment transport conditions and water discharge and might increase by up to 10 %. We conclude that the Lena Delta can be recognized as the global hot spot in terms of the hydrological consequences of climate change, which is altering sediment regimes, stream hydromorphology and carbon transport.

1. Introduction

In the largest periglacial Siberian rivers, the interactions between hydro-climatic factors and the deep permafrost introduce a pronounced specificity in terms of the climate change impact on the hydrological system of deltas. Recent studies show that continuous permafrost regions show increased flows throughout the Eurasian pan-Arctic (Feng et al., 2021). On the one hand, rising temperatures increase snow- or ice-melt. On the other hand, precipitation amounts and intensities might lead to highly concentrated surface runoff in the catchment area and changes in erosion, sediment transport and water chemistry. According to Syvitski et al. (2005), for every 2 °C of warming, a 30 % increase in the sediment flux could result, and for each 20 % increase in river discharge, a 10 % increase in sediment load could follow. The IPCC (Dentener et al., 2013) projected the rise of global-mean surface air temperature (SAT) from 1.4 °C to 5.8 °C by 2100. The discharge of the six largest Eurasian rivers would increase by 315 to 1 260 km^3 per year by 2100 (Shiklomanov et al., 2006), constituting an 18 to 70 % increase compared to present conditions. In their modelling study, Morehead et al. (2003) estimated that the sediment flux of six Arctic rivers would significantly increase in a range of up to 122 %. Furthermore, thawing permafrost releases additional sediments to erosion and transport. Predicted warming in the Arctic is expected to affect the extent of the permafrost and ice-covered regions, the amount of precipitation and the

* Corresponding author at: Faculty of Geography, Moscow, Lomonosov Moscow State University, Moscow 119234, Russia.
E-mail address: srchalov@geogr.msu.ru (S. Chalov).

https://doi.org/10.1016/j.ecolind.2023.111252
Received 28 June 2023; Received in revised form 6 November 2023; Accepted 8 November 2023
Available online 18 November 2023

productivity of terrestrial and aquatic ecosystems, which will affect river water and sediment discharges to the Arctic Ocean. The degradation of permafrost has recently led to increased runoff, erosion, and associated transport of total suspended matter and nutrients in the lower reaches of the largest Arctic rivers, which has a significant impact on biogeochemical cycles (Shakhova et al., 2007; Wild et al., 2019). Given recent findings that old permafrost-derived organic carbon plays an important role in aquatic ecosystems (Matsuoka et al., 2022), rapid warming is an important hydrological and ecological driver over northern high-latitude regions.

Even though the importance of permafrost thaw on hydrological processes is recognized widely (Vihma et al., 2019), the hydrological processes in the largest deltas of Arctic rivers still need to be considered, due to the complexity and costs of studying hydrological processes in these remote areas. Monitoring coastal systems is a challenging task, since these networks are costly to install and maintain. Delta zones of Arctic rivers have rarely been studied to date (primarily due to difficulties in access), resulting in a general lack of available data. In this regard, the particular exception is the largest Eurasian delta of the Lena River. Here, on Samoylov Island in the central Lena Delta, a Russian–German monitoring site connected to a research station was established in 1998. This monitoring site, together with yearly fieldwork on and around Samoylov Island and in other delta areas, has provided long-term data on, among other things, meteorological, hydrological, and permafrost conditions (Boike et al., 2019). Additionally, the PARTNERS and ArcticGRO programs (Holmes et al., 2012; McClelland et al., 2016a) provide year-round and interannual estimates of changing water composition at the delta apex. Recent field expeditions were carried out between 2005 and 2012 (Fedorova et al., 2015), and another in 2022 by Lomonosov Moscow State University (Chalov and Prokopeva, 2022), and these made numerous measurements of various hydrological parameters.

Long-term hydrological observations are processed at a few locations upstream from the delta and in the delta branches. Recent studies discussed the Lena River's annual discharge increase due to increasing winter flow, as well as increased streamflow and suspended and dissolved material release between the delta apex and branches from the ice complex (Juhls et al., 2020; Magritsky et al., 2018). Based on water temperature monitoring on the Bykovskaya channel, estimates of heat flux show an increasing trend from 1980 (Magritsky et al., 2018). Continuous measurements at Samoilov Island from 1998 to 2011 (Boike et al., 2013) detect no evidence of warming of mean annual air temperatures, and only winter air temperatures have warmed. Permafrost warmed by more than 1 °C at 10.7 m depth, which was related to changes in winter air temperature, net radiation, and snow cover. Through the integration of *in-situ* monitoring and remote-sensing data (Landsat), a long-term downstream increase along the distributary system of the Lena Delta was identified and attributed to higher discharges and the degradation of permafrost-dominated banks (Chalov et al., 2021; Chalov and Prokopeva, 2022, 2021). Consideration of these data led to the hypothesis that climatic and streamflow drivers (primarily air temperature, solar radiation, water discharges) may influence deltaic permafrost islands, which are increasingly being destabilized and contributing increased sediment load to streamflow along distributaries in the Lena Delta (Chalov et al., 2021). These processes might have important ecosystem impacts due to associated changes in carbon release, which covaries with sediment (Matsuoka et al., 2022). Understanding of climatic and streamflow drivers of sediment and carbon transport within the Lena River Delta requires the integration of climatic data accessible for this remote region and the identification of long-term historical hydro-climatic trends, which was considered the main goal of this paper.

The paper is based on an innovative integrated approach to capturing hydrological streamflow and sediment transport and quality records for the large Lena River that relies on the existing integrated toolboxes in hydrological studies (e.g., Chalov et al., 2017). Field, observational, remote-sensing, and climate reanalysis data are necessary resources to upscale across this scarce and poorly monitored region. To describe the weather conditions and climatic effects on streamflow and sediment pathways, we rely on ERA5 air temperature data, which is in good correlation with ground-based observations in the Arctic zone (Demchev et al., 2020). Our unique monitoring data and measurements present an opportunity to establish the first comprehensive estimate of the Lena River Delta climatic (precipitation, temperature, radiation, wind) and hydrological (water and sediment discharges) system in the early 21st century with a specific focus on long-term changes of riverine carbon, which is considered to be one of the most heavily impacted constituents of the Arctic biogeochemical cycle due to permafrost degradation and associated active-layer thickening. Therefore, to bridge current gaps in hydro-climatic change assessment for the Lena River Delta, we here investigate long-term hydroclimatic conditions of sediment pathways in this area, with the main objectives being to: (i) identify historical hydro-climatic trends based on ERA5 reanalysis, (ii) assess the current streamflow, sediment discharges, carbon (DOC and POC) concentrations and temperature trends at the delta top, and (iii) assess to what extent the observed trends are linked with the processes within the delta and how they affect the processes within the delta (primary, water distribution over delta distributary branches, suspended sediment budget). To the best of our knowledge, this is the first comprehensive study to integrate the issues of climate changes, sediment transport and water quality over large northern deltas. Our results yielded novel and essential data that could be used to estimate climate change consequences at the northern latitudes.

2. Data and methods

2.1. Lena delta. Site description

The Lena Delta's area is ~30,000 km^2 (Schneider et al., 2009) and includes a considerable number (over 6 000) of freshwater channels with a total length of 14 600 km (Ivanov et al., 1983) and approximately 29 500 lakes. The Lena Delta is situated in a zone of 500–600-m-thick continuous permafrost (Boike et al., 2013). The active (annually thawed) layer is 30–50 cm thick. The entire delta lies in the tundra zone except for the southern part of the delta. The four main distributaries represent the main sectors of the channel structure: the largest is the Trofimovskaya branch that flows north-east into the Laptev Sea; the second-largest branch by water discharge is the Bykovskaya branch that turns sharply to the east after Stolb Island and flows into the Buor Khaya Gulf; the third- and fourth-largest distributaries are the Olenekskaya branch that flows west into the Kuba Gulf and the Tumatskaya branch that flows north into the Laptev Sea (Fig. 1). The shoreline length from the Olenekskaya branch mouth to the Bykovskaya branch mouth is ~193 km, and the total length of the river network is 14 600 km.

2.2. Climatic data

In this paper three sources of climatic information were used:

1) **Stations of the Russian Federal Service for Hydrometeorology and Environmental Monitoring** (Roshydromet) in Tiksi and Kyusyur, provided by the Russian Research Institute of Hydrometeorological Information – World Data Center. Tiksi station is located 115 km from Stolb Island and 20 km from Neelova Bay, into which the Bykovskaya channel flows, and provides air temperature monitoring data from 1930 and precipitation data from 1933. The Kyusyur station is located 194 km upstream from Stolb Island and provides air temperature and precipitation data from 1925. The length of the data series reaches 113 years (with 9 years missing from 1917 to 1925) for the Kyusyur station and 92 years for the Tiksi station.
2) **Reanalysis ERA5-Land datasets**. The ERA5-Land dataset is available for free public use for data covering the period from 1950 to 2–3

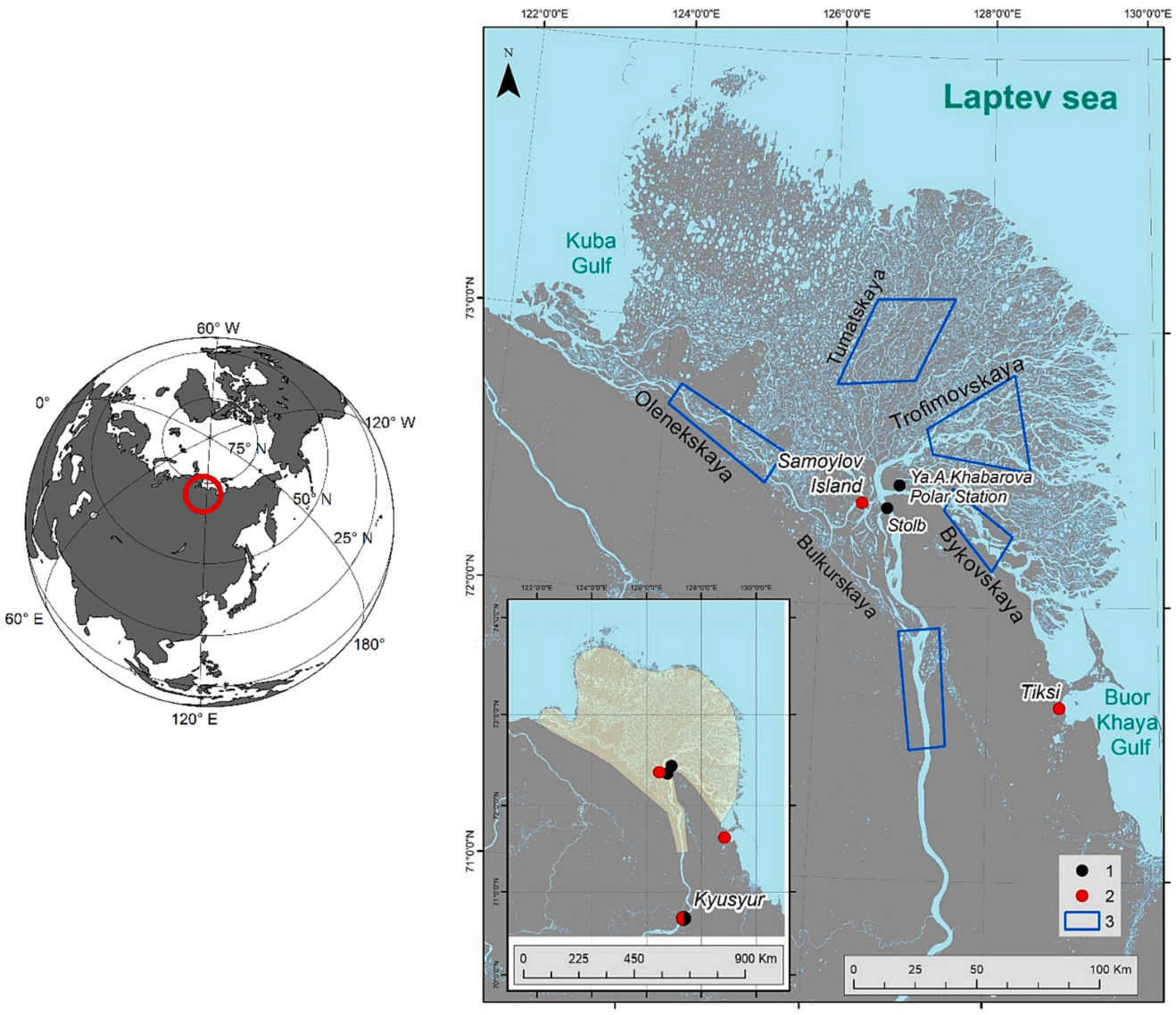

Fig. 1. The Lena Delta study area: 1 – gauging stations; 2 – meteorological stations; 3 – areas for calculating average sediment concentrations representative for particular sectors of the delta (see details in the text); yellow area – ERA5 reanalysis application for Lena Delta.

months before the present at a spatial resolution of ~9 km (Muñoz-Sabater, 2019). Four ERA5 meteorological variables were used in this study: 2-meter air temperature (°C); total precipitation (mm); surface net solar radiation ($W \cdot m^{-2}$) and 4) wind speed ($m \cdot s^{-1}$). Other components of the hydrological system, and in particular sediment transport, are most affected by these variables during the ice-free period (June–September). ERA5-Land hourly data from 1950 to the present were downloaded in NetCDF format from the Copernicus Climate Data Store (https://cds.climate.copernicus.eu/cdsapp#!/dataset/reanalysis-era5-land?tab=overview). The daily datasets were compared and tested for agreement with observational data from Kyusyur and Tiksi stations. The correlation coefficient between ERA5-Land and Tiksi air temperatures was 0.93, and 0.92 between ERA5-Land and Kyusyur station air temperatures (Supplementary 1).

Two-meter air temperature (K) was converted to °C and hourly data was converted to average day values, and these are further used to compare against sediment transport patterns revealed for particular days. The duration of the temperature dataset is 72 years.

Surface net solar radiation is the difference between downward radiation (amount of solar radiation, also known as shortwave radiation) reaching the surface of the Earth (both direct and diffuse) and reflected solar radiation (amount reflected by the Earth's surface, which is governed by the albedo). This variable too has been gathered from the beginning of the forecast time to the end of the forecast step for the ERA5-Land reanalysis dataset.

The wind speed monitoring data provide a u-component (eastward component) and a v-component (northward component) of wind, which were converted to wind speed in m s^{-1} as described in Supplementary 2 Eq. (1).

The following characteristics of the ERA5-Land data series and their changes were calculated:

- minimum, mean and maximum values of 2 m air temperature, precipitation, surface net solar radiation and wind speed over 72 years (from 1950 to 2021) and for the months of the open-water period (June–September);
- the Pettitt test, which was applied to calculate the year of the beginning of significant climatic changes (Pettitt, 1979). The Pettitt test is a non-parametric test that has been used in a number of hydroclimatological studies to detect abrupt changes in the mean of

the distribution of the meteorological variable (Mallakpour and Villarini, 2016). The description of the test is presented in Supplementary 2–2.

- Linear trend with an estimate of the confidence interval at 95 % significance level for the period of climate change using the non-parametric Spearman's rank correlation coefficient (Spearman's RCC)(Naghettini, 2016) (Supplementary 2–3).

3) **Soil Temperatures**. Soil and permafrost temperature monitoring data were used from the long-term observatory on Samoylov Island (Boike et al., 2019). Here, meteorological parameters and energy balance have been recorded since 1998 and subsurface permafrost temperature since 2006. We used surface (t_0) and 0.75 m ($t_{0.75}$) soil temperatures taken from a measurement chain of temperature sensors installed in a permafrost borehole down to a depth of 22 m at Samoylov Island (Fig. 1). Daily means were calculated from hourly measurements. Permafrost temperature and active-layer thaw depth data were downloaded through the Global Terrestrial Network for Permafrost (GTN-P) database (http://gtnpdatabase.org). The dataset lacks data for the period from June to September. No data are available for the period from 1 June to 24 August in 2006, from 1 August to 30 September in 2015 and from 20 September to 30 September in 2008 and 2021.

Additionally, we calculated accumulated sums and means of air temperature, soil temperature at the soil surface and 0.75 m depth, precipitation, solar net radiation, and wind speed variables over 3, 5, and 7 days (Supplementary 2–4).

2.3. Hydrological data

Long-term hydrological variability was analyzed based on discharge from the Kyusyur gauging station, which characterizes inflow rates to the Lena Delta. Here, the upstream watershed covers 2 430×10^3 km^2, the delta apex is located 145 km downstream, and the sea (the mouth of the Bykovskaya channel) is 315 km downstream. Water level (H), water discharge (Q) and water temperature (T) have been measured at Kyusyur since 1934, and suspended sediment concentration (SSC) and suspended sediment discharge (R) since 1960. Within the delta, long-term observations were made at the gauging station upstream of the Bykovskaya channel (see Fig. 1) located on the main channel between the delta apex and Stolb Island. The "Stolb Island" polar station has been operating here since the 1950 s (the station is now named "Yu. A. Khabarov").

We compiled a database of daily, mean monthly, and mean annual water levels and discharge for the period 1935–2020 from the Kyusyur gauging station and for 1950–2020 from the Yu. A. Khabarov gauge. Decadal and monthly suspended sediment concentration and average monthly and annual discharges of suspended sediments were analyzed for 1936, 1944, and 1960–2010 at Kyusyur and for 1968–2007 at Khabarov station. Decadal and monthly water temperatures were analyzed for 1935–2019 and 1951–2012. The gaps in the streamflow time-series at the Kyusyur gauge (2012–20) were filled by using separate empirical relationships between water discharges Q_{month} and water levels H_{month} (correlation coefficients of 0.9 to 0.99) for each of the individual or pairs of months May, June–July, August–September, October and the remaining winter months.

The gaps in the time-series of average monthly sediment discharges were filled by using average monthly water discharges and the power regression $R = aQ^b$, where $a = 5.35\times10^{-6}$, $b = 1.8$ ($R^2 = 0.92$) for May–June and $a = 1.09\times10^{-6}$, $b = 2.02$ ($R^2 = 0.60$) for July–October, for data since 1988 (Magritsky, 2015). The annual values of suspended sediment discharge W_R (million tons/year) were calculated for Kyusyur gauging station. The temporal homogeneity of the time-series was verified using the Fisher (*F-test*), Student (*t-test*), and Mann–Whitney (*U test*) tests for time-correlated and asymmetric series of hydrological characteristics. Independence hypotheses were tested using the Andersen test and the test of the number of series (Supplementary 2–5).

Additionally, water temperature records from both gauges were used to calculate the heat flux W_T as:

$$W_T = c_p \rho T W \quad (1)$$

where c_p is water specific heat capacity (kJ·kg^{-1}•°C^{-1}), ρ is the density of water (kg·m^{-3}), T is the average water temperature per decade (°C), and W is the volume of water runoff (m^3) per decade. The values of heat runoff for the particular seasons and annual values ($W_{T,a}$) were calculated as a sum of 10-day averages.

The Arctic Great Rivers Observatory (ArcticGRO; https://arcticgreatrivers.org/, accessed: 30 April 2023) dataset from Zhigansk gauging station was used to evaluate long-term riverine carbon entering the Lena Delta. This dataset provides data on hydrology and biogeochemistry of the greatest (largest) Arctic rivers (Ob, Yenisei, Lena, Kolyma, Yukon, and Mackenzie) since 2003 at an irregular sampling frequency. Samples represent different hydrographic stages and seasons, with particular emphasis on depth-integrated sampling (for details and protocols, see McClelland et al., 2016b). The database used in our estimates included 87 DOC and POC measurements taken between 12 August 2003 and 25 November 2021 (an average of ~5 samples per year). We assume that the Zhigansk gauging station, which is located ~800 km upstream from the Lena Delta, may not be entirely representative of the discharge to the delta but provides approximate values.

Data on suspended sediment concentration (SSC, mg·L^{-1}) was collected during comprehensive fieldwork in the Lena Delta conducted from 10 to 16 August 2022. Here, water samples were taken with a filterless submersible 12 V pump from three layers (surface, mid-section, and near-bottom) to account for the vertical distribution of the suspended sediment. For SSC determination, water samples were filtered through pre-weighed and pre-dried (at 105 °C for two hours) membrane filters (pore size 0.45 μm) from the "Millipore" filtration system. The filter samples were then oven-dried (at 105 °C for two hours) and reweighed to determine SSC. The mass of dry sediment was determined by gravitational difference. The SSC was deduced from the measured mass of dry sediment and water sample volume:

$$SSC = \frac{m_2 - m_1}{V} \quad (2)$$

where m_2 is the mass of filter and dried residue (mg), m_1 is the mass of clean filter (mg), and V is the volume of water sample filtered (L) which is defined based on the amount of the sediment in the sample (on average, 2 L). The mass of the membrane filter and wet sediment were measured with a precision of ±0.001 g.

Water sampling for suspended sediment analyses sampling was coupled with simultaneous discharge measurements made using a Teledyne RDInstruments (TRDI) RioGrande WorkHorse 600 kHz ADCP unit mounted on a moving boat. For each sample in a depth profile, the boat was repositioned at its original location and sampling was performed while drifting at the river water velocity. In total, 24 cross-sectional measurements were made in the Bykovskaya, Bulkurskaya, Olenekskaya, Tumatskaya, Arinskaya branches and in the Main Channel (Fig. 2) and aimed to quantify the flow partitioning between delta distributaries. The relative discharges in the particular distributaries of the delta were calculated as:

$$Q_i\ (\%) = Q_i/Q_0 * 100\ \% \quad (3)$$

where Q_i is the discharge (in m^3·s^{-1}) in an individual distributary and Q_0 is the total discharge (in m^3·s^{-1}) of the Selenga prior to entering the delta.

2.4. Remote-sensing data

Additionally, long-term changes (between 1999 and 2022) of suspended sediment transport behavior within the delta were retrieved

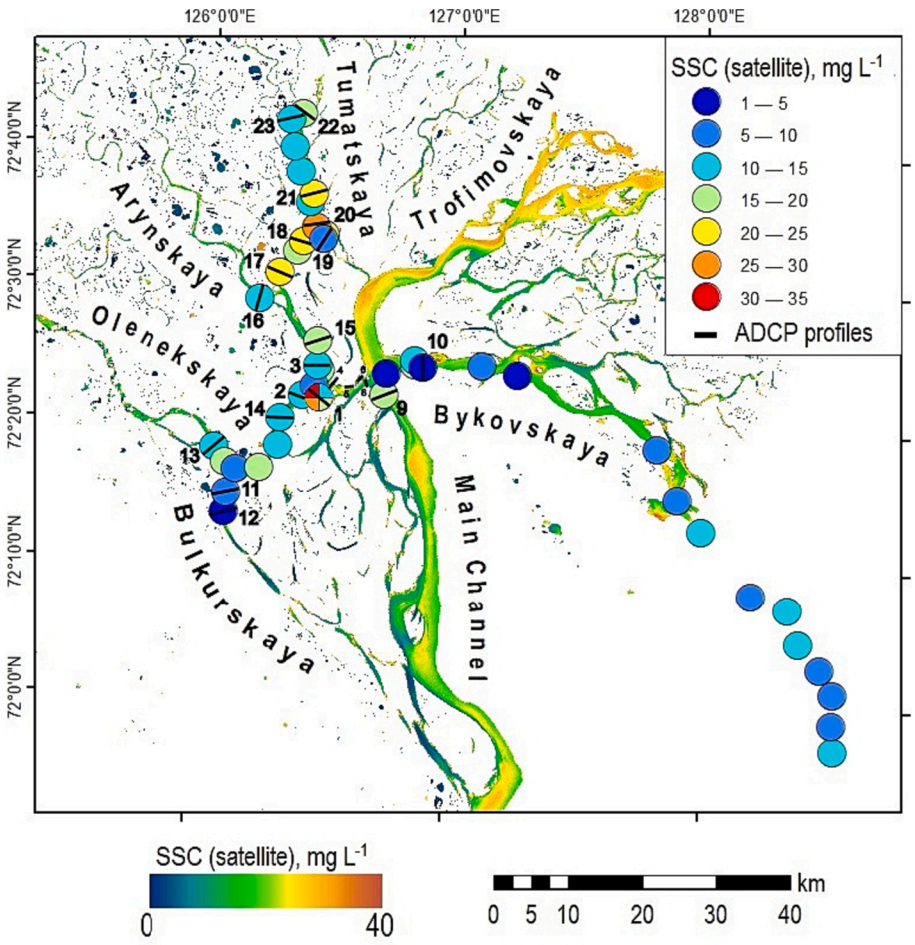

Fig. 2. Measured surface sediment concentrations and water discharges from 10 to 16 August 2022 plotted against satellite-derived (Landsat image from 16 August 2022) SSC map in the upper part of the Lena Delta.

from remote-sensing applications (Chalov et al., 2021; Chalov and Prokopeva, 2022). The SSC was calculated from reflectance intensities (ρ) of Landsat images and based on the relationships with SSC data obtained during the field campaign in the Lena River Delta (32 measurements) connected with the available image from 16 August 2022 ($R^2 = 0.76$):

$$SSC = 1512.1 * \rho_{red} - 25.0 \quad (4)$$

where ρ_{red} is bottom of the atmosphere reflectance in the red band (Landsat 8).

Landsat Collection data products were downloaded from the USGS Earth Explorer website from 2000 to 2022 for the Lena Delta. A total of 75 Landsat images for ice-free periods between June and October from 2000 to 22 were used. Suspended sediment concentrations (SSC, $mg \cdot L^{-1}$) were determined in the Lena River main channel and four deltaic branches: the Bykovskaya, Trofimovskaya, Tumatskaya, and Olenekskaya channels (for additional details, see Chalov et al., 2021; Chalov and Prokopeva, 2022). The images were atmospherically corrected using the SIAC method to remove the effects of atmospheric scattering from an image. SIAC has shown good performance for land surfaces (Yin et al., 2022) and inland water bodies (Sherjah et al., 2023).

Each of the four channels and river upstream from the delta were characterized by an average suspended sediment concentration (SSC) within the selected areas (see Fig. 1), which was estimated for all pixels classified as "water". The non-water pixels were excluded from analyses based on NDWI index and manual classifications. The SSC was calculated as average for particular areas within the delta (shown in Fig. 1 as blue polygons) and refer to near-surface suspended sediment concentrations (approximately 1 m from the water surface (Chalov et al., 2021; Pavelsky and Smith, 2009).

For each of four deltaic branches, SSC change (ΔS_0) was calculated on the basis of the difference between SSC at the upstream area (upstream from the delta, SSC_1) and downstream area (within the particular branch, SSC_2):

$$\Delta S_0 = SSC_2 - SSC_1 \quad (5)$$

Relative sediment changes ΔS (%) were calculated as:

$$\Delta S = \Delta S_0 / SSC_1 \quad (6)$$

Three possible ratios between sediment input and output were analyzed: $SSC_2 > SSC_1$, $SSC_2 < SSC_1$, and $SSC_2 \approx SSC_1$, which correspond to either an increase ($\Delta S > 0$) or a decrease ($\Delta S < 0$) in sediment concentrations. These changes are attributed to variations in suspended sediment concentration in the near-surface layer, which is taken as an assumption in our calculations. In particular, we consider that changes in average sediment concentration in the channel profile might be different from those calculated with the above-mentioned methodology.

The ΔS (6) dataset was compared with observed weather conditions (air temperature, radiation, wind) and streamflow inputs to the delta in the period 2000–22. The critical factors influencing sediment load within the delta were identified using correlation analysis, and the corresponding quantitative relationships were established.

3. Results

3.1. Climatic changes in the Lena delta

The trends in air temperatures from reanalysis ERA5-Land datasets are summarized in Table 1. The results suggest a shift toward a warmer climate. Air temperatures increased significantly (p-value < 0.05) according to the Pettitt test. An increase in warming rate was observed between the periods 1950–99 and 2000–21, i.e., the most significant increase in air temperature occurred in the last 20-year period (Table 1). Average air temperatures were 4.1 °C for the period 1950–99, whereas for the last 20-year period (2000–21) it reached 6.0 °C. Tiksi and Kyusyur weather station's air temperature series based on the Pettitt test also show significant changes in air temperature, with a shift to more rapid warming in 2001 for Tiksi and in 2004 for Kyusyur (p-value < 0.05).

The rate of air temperature rise was 0.86 °C per decade from 1979 to 2021. The subsequent period (2000–21) warmed at 1.61 °C per decade. The significances of the trends by the non-parametric Spearman rank correlation coefficient (1979–2021) were 0.63 and 0.67 at p-value < 0.05 (Fig. 3a), respectively.

The change in warming rate since 2000 was not uniform across the delta. The color-coded map in Fig. 4 shows how average air temperature trends changed. The maximum warming rate reaches 2.11 °C per decade. Higher rates are mainly found in the delta's eastern part, near the Bykovskaya channel mouth and along the ridges in the southern part of the delta. Trend values also increase in the south-western part of the delta, along the Olenekskaya channel. The lowest change rates (1.66 °C per decade) are observed in the central delta, where air-mass penetration from the Laptev Sea is most likely to have a cooling effect. The value of the trend from 1992 to 2021 in the delta area is lower than the values over the last 20 years (2004–21). In general, as in 2004–21, the higher values of the 1992–2021 trend were observed in the southern part of the delta, with minimum values in the central and northern parts of the delta.

Surface net solar radiation significantly increased from 110 $W{\cdot}m^{-2}$ (from 1950 to 1992) to 118 $W{\cdot}m^{-2}$ (from 1993 to 2021) (Fig. 3b). The value of coefficients for 2004–21 is 0.48, but the Spearman rank correlation for the first part of warming (1991–2004) is not significant at p-value < 0.05. Rising surface solar net radiation was 2.64 % per 10 years from 1992 to 2021 and 6.99 % per ten years from 2004 to 2021.

According to the Pettitt test, there were no significant trends in rainfall (p = 0.9026) and wind speed values (p-value is 0.145) (Fig. 3c and d). However, non-significant trends were recorded: one upward at the end of the 1980s and one downward from the end of the 2000s. Also, significant statistical changes have not been established for precipitation series at Tiksi and Kyusyur weather stations.

Soil temperature from the observations on the Samoylov Island (Boike et al., 2019) displayed a general increasing tendency, with the higher values after 2017 (Fig. 3e). Compared to t_0, soil temperature at 0.75 m exhibited more stable values over time (Fig. 3f).

Table 1
Results of trend analyses of air temperature, total precipitation, surface net solar radiation and wind speed in 1950–2021 based on ERA5-Land reanalysis data.

Meteorological variables	Change year (according to Pettitt test [1])	*p*-value	Mean before	Mean after
air temperature	2000	0.0000*	4.1 °C	6.0 °C
total precipitation	1977	0.9026	170 mm	160 mm
surface net solar radiation	1992	0.0132*	110 $W{\cdot}m^{-2}$	118 $W{\cdot}m^{-2}$
wind speed	1983	0.145	4.86 $m{\cdot}s^{-1}$	4.98 $m{\cdot}s^{-1}$

* Statistically significant (i.e., p-value < 0.05).

3.2. Streamflow input to the delta and partitioning across delta distributaries

The water input to the delta is characterized by the 17,200 $m^3{\cdot}s^{-1}$ average long-term water discharge of the Lena River at the Kyusyur gauging station (543 km^3 per year average annual runoff W_a) for the period 1927–2020. These average numbers include linearly interpolated numbers for the years 1927–34 and 2012–20 from the water stage measurements. The streamflow is characterized by relatively small interannual variability (coefficient of variation Cv = 0.12) and high correlation (r[1] = 0.32). The Anderson test t(A) = 3.2 (+) and the test of the number of series t(u) = 2, 12 (+), which are normal for very large rivers, were applied. Wet-dry cycles of water flow are identified (Supplementary 3), among which there was a long dry period in 1939–57 (with the average value of the difference-integral curve (k_{av} = 0.91), medium flow in 1958–2003 (k_{av} = 0.99) and the modern high-water period in 2004–20 (k_{av} = 1.10). The results show an increasing trend in streamflow since 1988 (Spearman's rank correlation coefficient [RCC] [+]) and a particularly large increase in W_a since 2004. W_a increased by 56.3 km^3 per year for the period 1988–2020 compared to 1935–87.

The hydroclimatic changes of the streamflow input to the delta may have a significant impact on hydrological conditions across the delta, especially on flow partitioning between delta distributaries and sediment dynamics. Flow partitioning has rarely been investigated due to the delta's remoteness and size. We collected data of repeated point measurements of water discharge at key locations over the delta. These data include water discharge measurements taken on 12–13 August 2022 (see Fig. 2 and Supplementary 4) and observations reported by Bolshiyanov et al. (2013), Fedorova et al. (2015), and Magritsky et al. (2018). The dataset reveals constant flow partitioning. Over the last 20 years, flow partitioning between main distributaries has remained mostly unchanged: of the Lena's flow input to the delta, approximately 24.9–25.0 % is directed to the Bykovskaya branch, 58–59.2 % to Trofimovskaya, 6 % to Tumatskaya, and 6.6 % to Olenekskaya. The difference ratio between various discharges (Bolshiyanov et al., 2013; Magritsky et al., 2018) is less than 0.3 %.

The average annual heat runoff ($W_{T,a}$) of the Lena river is very large (at the Kyusyur gauging station: $16\,120\times10^{12}$ kJ per year for 1935–2019), despite the low water temperatures (average annual T_{june} = 5.2, T_{july} = 14.2, T_{aug} = 12.7 and T_{sept} = 6.3 °C) and a short warm season (ice-free period from June 4 to October 13). This phenomenon is explained by the huge discharge and its increase during the warm season. W_a and $W_{T,a}$ were closely linked (R^2≈0.52). This correlation improves if we take into account the water temperature (R^2≈0.72):

$$W_{T,a}(\mathrm{kJ}\times10^{15}) = 0.028W_a + 1.416\overline{T}_{june-sept} - 12.9 \quad (7)$$

In Eq. (7), $\overline{T}_{june-sept}$ is the average water temperature for ice-free June–September. It can be replaced by the corresponding air temperature ($\bar{t}_{june-sept}$) at the Zhigansk and Kyusyur weather stations (R^2≈0.66):

$$\overline{T}_{june-sept} = 0.584\bar{t}_{june-sept}(\mathrm{Zhigansk}) + 0.231\bar{t}_{june-sept}(\mathrm{Kyusyur}) + 1.2 \quad (8)$$

The Lena River heat runoff obtained from measurements at the Kyusyur gauging station is underestimated due to the cooling effect of the waters from right-bank tributaries – by about 1 015 kJ per year (Magritsky et al., 2018). The heat runoff of the Lena River is growing due to an increase of water discharges (since 1988) and water temperature (especially since 1997) (Spearman's RCC [+]) (Fig. 5). The difference in $W_{T,a}$ between the periods 1988–2019 and 1935–87 was 1 480 kJ per year, or 9.5 %. The increases in water temperature in June, July–August and September were 1.1, 0.6 and 0.05 °C, respectively. There are the same trends in heat flux within the delta. The relationship between the average monthly water temperatures at the Kyusyur and Khabarov gauging stations is close (R^2 from 0.63 to 0.77). The duration of the

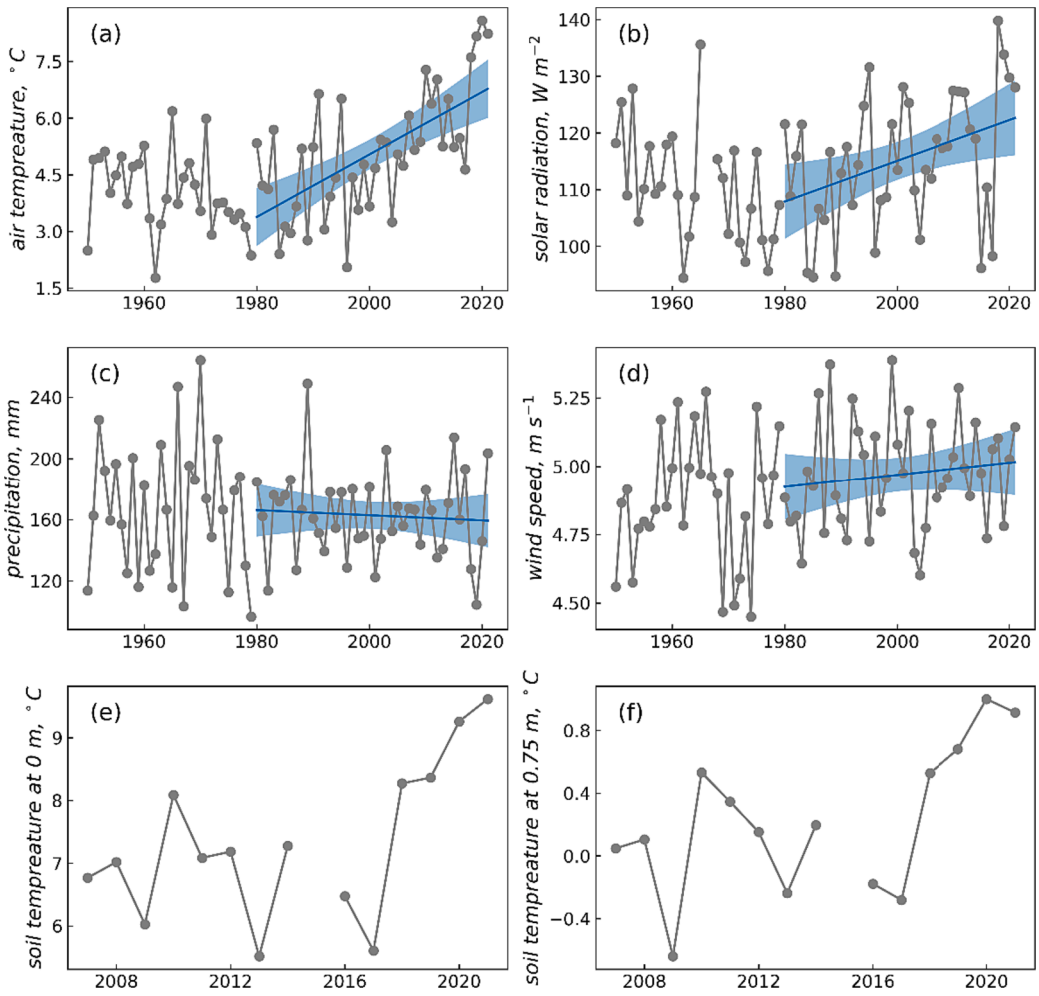

Fig. 3. Long-term changes in mean air temperature (a), surface net solar radiation (b), precipitation (c), wind speed (d) (based on ERA5-Land reanalysis data), soil temperature at 0 m depth (e), soil temperature at 0.75 m depth (f) in the Lena Delta. For a–d, the overall linear trend for 1979–2020 is shown (blue line), with its 95 % confidence interval.

period with T ≥0.2 °C has increased by 8 days over the last 30 years (1988–2019).

3.3. Sediment load

During the observation period, the annual sediment runoff at Kyusyur varied between 7.6 (1984) and 53.6 million tons (2005). Runoff and sediment hydrograph coincide to some extent over the long term. There are two trends in annual sediment discharge: W_R decreased until 1986–1987 and increased, although at a statistically insignificant rate, in subsequent years by an average rate of 6.1 million tons per year (significant only in the *U* test [+]) (see descriptions in Supplementary 2). Average annual water flow and sediment runoff exhibit a moderate correlation (R^2≈0.25). As far as sediment conveyance depends on precipitation and water discharge (Costard et al., 2003), these changes can be attributed to snowmelt flood having decreased from 82.7 % in 1936, 1944, 1960–87 to 64.8 % in 1988–2010, and the low-water period contribution to annual flow having increased from 16.8 to 34.9 %. The uniformity of a number of low water values of sediment load was violated both by variance (F-test [+]) and by mean (*U* test [+]) (for descriptions of test, see Supplementary 2).

Satellite image analysis on the Lena River Delta channels shows that suspended sediment load both increases and decreases along the main distributaries of the delta (Fig. 6). During June (end of spring freshet season), at the end of July, and in August, sediment concentrations tend to increase (ΔS >0), which implies net erosion along the channels. However, during other open-flow conditions, sediment concentrations mostly decrease, which implies net deposition. These changes can be attributed to the water discharges conditions and elevation levels, as well as other hydroclimatic (wind, permafrost thaw) and in-channel (bank erosion) conditions. The whole dataset provides evidence that a downstream sediment transport increase ($\Delta S > 0$) dominates in the Trofimovskaya branch. Here, the downstream increase in surface sediment concentration (for example, from 45 mg·L^{-1} in the main channel to 60 mg·L^{-1} in the Trofimovskaya branch) occurred in 75 % of the observed images. Net deposition is observed at the other three distributaries. In particular, the average relative sediment change ΔS was ⁻22.7 % along the Tumatskaya branch and ⁻8.96 % along the Olenekskaya branch (a decrease in SSC from 1 mg·L^{-1} in the main channel to 6 mg·L^{-1} in the Olenekskaya channel).

The relationships of relative sediment changes ΔS (%) with climatic parameters are given in Table 2. Relative suspended sediment changes ΔS (%) are constant during the period from 2000 to 2022 and do not correlate to Lena River discharge (see Fig. 6, Supplementary 5 for additional details). As for precipitation datasets, high values of correlations (r >0.7) were found only between these parameters and ΔS (%) in the left Olenekskaya branch, but the correlation is not significant according to Student's *t*-test at the level of α = 5 % due to the shortness of the dataset. For the other parts (Trofimovskaya and Tumatskaya) of the delta, the values of the linear relationships between precipitation

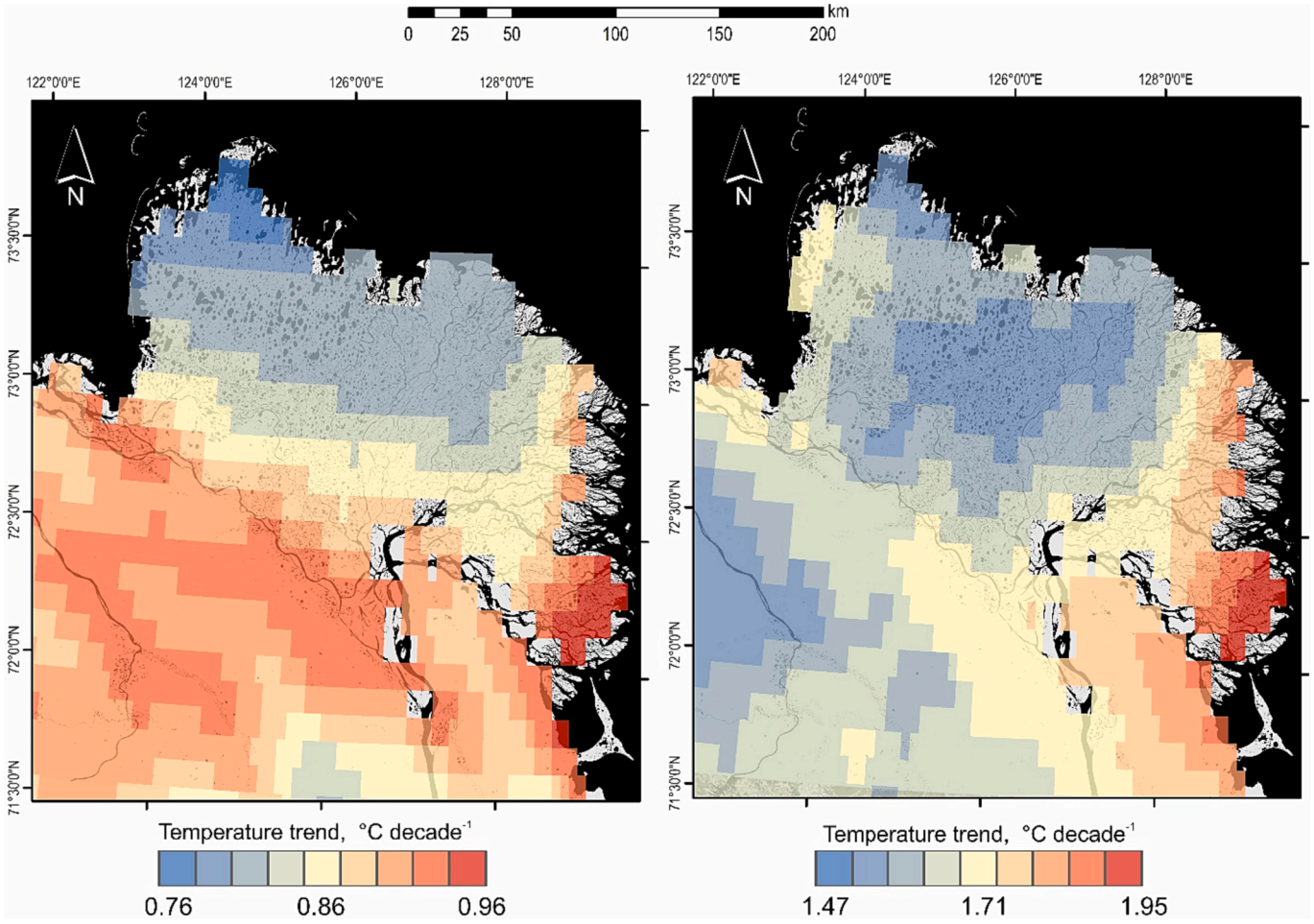

Fig. 4. Map of air temperature trend values in the Lena River Delta: *left* – from 1979 to 2021, *right* – from 2000 to 2021. * Note value ranges represented by color bars differ between maps.

and ΔS were less but moderate (r >0.3). Only for the Bykovskaya distributary system was a negative relationship (and no significant correlation) with daily precipitation (r=⁻0.22) found. Sediment load changes are most sensitive to changes in daily wind speed ($m \cdot s^{-1}$), in particular 3-day and 5-day average wind speeds, as indicated by significant moderate correlations (r >0.3) across all four major distributaries. Additionally, the subsurface change has the greatest effect on increasing streamflow in the Tumatskaya and Olenekskaya branches: daily soil temperature at the depth of 0.75 m (Tsoil 0.75 m) and sums over 3 (∑3d Tsoil [0.75 m], °C) and 5 (∑5d Tsoil [0.75 m], °C) days are correlated with streamflow discharge.

List of parameters:

1) daily air temperature (Tair) and sums over 3 (∑3d Tair, °C), 5 (∑5d Tair, °C) and 7 (∑7d Tair, °C) days;
2) daily precipitation and mean over 3, 5 and 7 days;
3) daily wind speed and mean over 3 and 5 days;
4) daily solar radiation (SR) and sums over 3 (∑3d SR, $W \cdot m^{-2}$), 5 (∑5d SR, $W \cdot m^{-2}$) and 7 (∑7d SR, $W \cdot m^{-2}$) days;
5) daily soil temperature on the surface (Tsoil 0 m) and sums over sums over 3 (∑3d Tsoil [0 m], °C), 5 (∑5d Tsoil [0 m], °C) and 7 (∑7d Tsoil [0 m], °C) days;
6) daily soil temperature at depth 0.75 m (Tsoil 0.75 m) and sums over 3 (∑3d Tsoil [0.75 m], °C), 5 (∑5d Tsoil [0.75 m], °C) and 7 (∑7d Tsoil [0.75 m], °C) days;
7) delta topset water daily discharge given lag time from Kyusyur to the top of the delta (2 days).

Overall, multilinear regression showed that sums of daily air temperature and wind speed over 3 days make the most pronounced contribution to ΔS variation. However, for the main branch, Trofimovskaya, this connection is not significant ($R^{2=}$0.09) according to F-test (p-value < 0.05). For other branches, close connection applies only if $\Delta S > 0$ (Fig. 7) and total $R^{2=}$0.22–0.23.

3.4. Carbon riverine transport

The ArcticGRO dataset (see section 2.2) was used to estimate carbon dynamics entering the delta since 2003. POC ($mg \cdot L^{-1}$) and DOC ($mg \cdot L^{-1}$) concentrations correlate with observed daily values of Q (corrected for distance between Zhigansk and Kyusyur) and SSC at Kyusyur gauging station (Table 3). POC mostly depends on sediment transport conditions, but also exhibits a relationship with water discharge. DOC is mostly driven by water discharge, whereas SSC might induce a secondary impact through hydrogeochemical conditions of carbon mineralization. The significant relationship for POC ($R^2 = 0.93$) is:

$$POC = 0.1245 + 7.4*10^{-6}*Q + 0.015*SSC \quad (9)$$

DOC was approximated as a function of Q and SSC ($R^2 = 0.55$):

$$DOC = 6.44 + 10^{-4}*Q - 0.018*SSC \quad (10)$$

DOC and POC *in-situ* data vary greatly interannually and seasonally (Fig. 8). The concentrations are highest in spring after the ice break-up and lowest in dry summer months and during the winter low-water

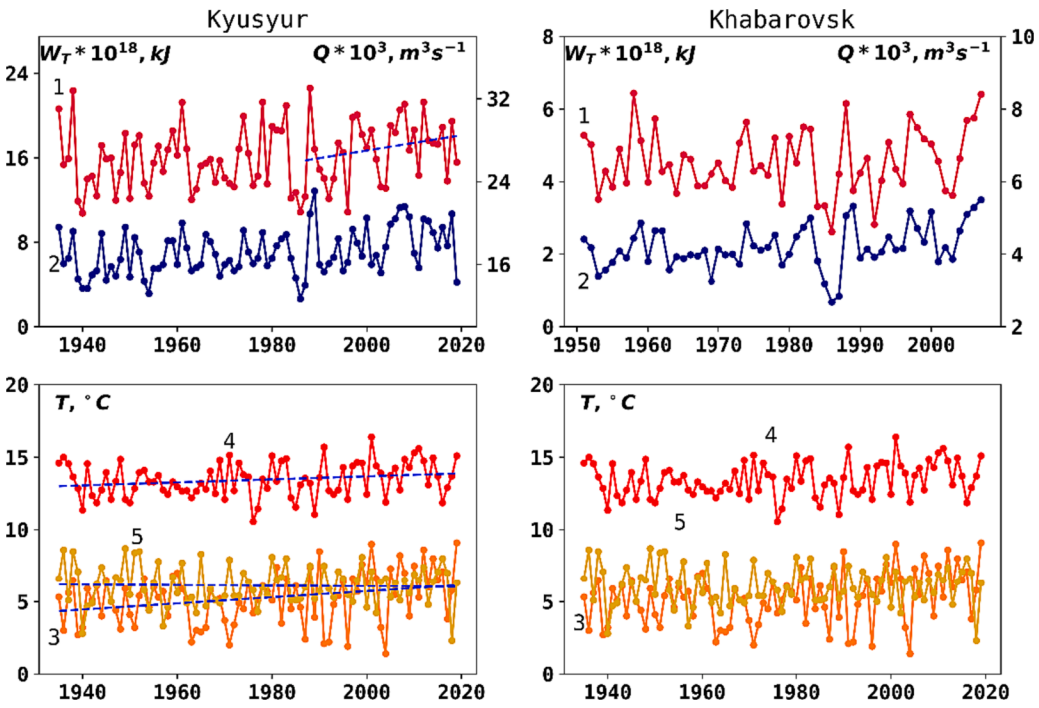

Fig. 5. Long-term fluctuation in the average annual flow of heat (1), discharge (2), and average water temperature for June (3), July–August (4), and September (5) at the Kyusyur (a) and Khabarov (b) gauging stations.

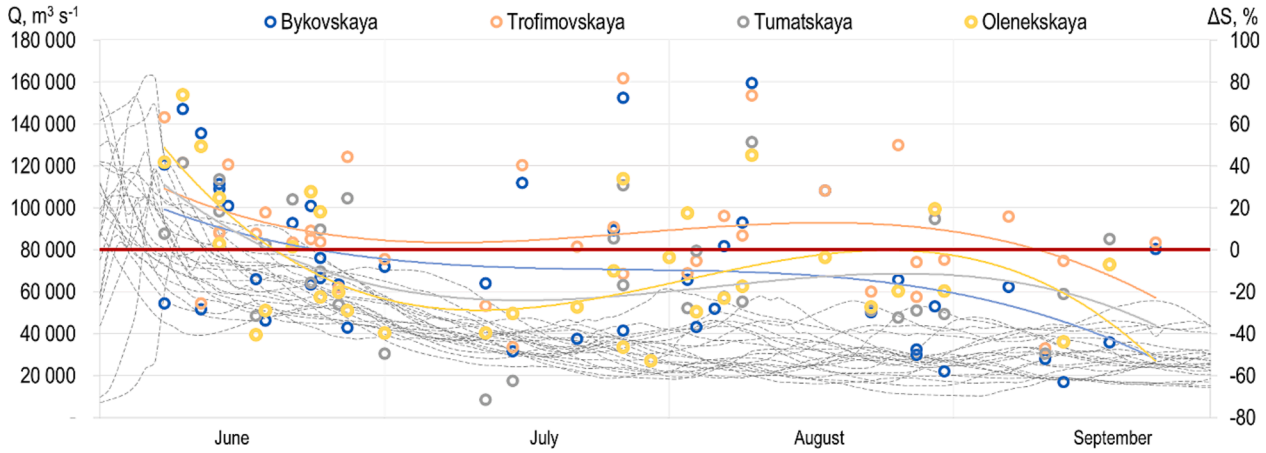

Fig. 6. Seasonal changes in suspended sediment transport ΔS along 4 major distributaries of the delta (based on Landsat data from 2000 to 2022). Dashed gray lines represent water discharges (Q, $m^3 \cdot s^{-1}$) on Kyusyur station; solid lines show cubic polynomial regression of suspended sediment (ΔS, %) values.

period. The Mann–Kendall test and Wald criteria were applied to DOC and POC series to detect a trend. DOC did not show a significant change, partly due to the relative shortness of the period (2003–21) of observations. Based on Mann–Kendall and Wald criteria, there is no significant interannual variability of DOC changes (p-value = 12–13 %) for this relatively short period (2003–21). Conversely, the POC substantially decreased over the studied period (p-value = 0.007–0.008 %) up to ⁻10.7 % per year.

4. Discussion

4.1. Responses of weather conditions, streamflow, and sediment load to climate change

Our study suggests that the Lena Delta has recently demonstrated a shift to more rapid warming. These results were obtained from the ERA5 reanalysis dataset, which is more representative of the whole Lena Delta compared to meteorological stations, since the delta is bounded by high ridges that can impede continental air masses. The predominance of winds from the north and north-east in the summer months can also have impacts that vary locally.

The results of climatic assessments based on ERA5 correlate well with regional observations. According to results based on four observational datasets (NASA's Goddard Institute for Space Studies Surface Temperature version 4 [GISTEMP], the Berkeley Earth temperature dataset [BEST], the Met Office Hadley Centre/Climatic Research Unit version 5.0.1.0 [HadCRUT5] and ERA5 reanalysis), the Arctic region has been warming since 1979 (Rantanen et al., 2022). A previous study (Demchev et al., 2020) showed that, in the coastal zone for May–October, ERA5 overestimates air temperature by an average of 0.29 °C and has a random error of 2.28 °C for daily values. The corresponding values for November–April are 0.27 °C and 2.9 °C. Over the Arctic region, the

Table 2
Correlation matrix between various climatic parameters and SSC change over Lena Delta (Significant correlations according to Student's *t*-test at the level of α = 5 % are highlighted in bold.).

Parameters	ΔS, %			
	Bykovskaya	*Trofimovskaya*	*Tumatskaya*	*Olenekskaya*
Daily Tair, °C	0.26	0.11	0.04	0.18
∑3d Tair, °C	0.28	0.07	0.10	0.27
∑5d Tair, °C	**0.31**	0.12	0.12	0.33
∑7d Tair, °C	**0.32**	0.19	0.12	0.32
Daily P, mm	−0.22	0.36	0.46	0.77
3-day precipitation (mean), mm	−0.13	−0.07	0.04	0.53
5-day precipitation (mean), mm	−0.21	−0.33	−0.11	0.24
7-day precipitation (mean), mm	−0.29	−0.27	−0.26	0.03
Daily wind, $m \cdot s^{-1}$	**0.34**	0.22	**0.59**	**0.43**
3-day wind (mean), $m \cdot s^{-1}$	**0.37**	**0.40**	**0.58**	**0.44**
5-day wind (mean), $m \cdot s^{-1}$	**0.34**	**0.32**	0.35	**0.34**
Daily SR, $W \cdot m^{-2}$	**0.37**	0.19	0.17	0.17
∑3d SR, $W \cdot m^{-2}$	**0.38**	0.20	0.29	0.26
∑5d SR, $W \cdot m^{-2}$	**0.40**	0.20	0.25	0.32
∑7d SR, $W \cdot m^{-2}$	**0.40**	0.22	0.26	0.29
Tsoil (0 m), °C	0.15	−0.06	−0.12	0.07
∑3d Tsoil (0 m), °C	0.12	−0.09	−0.04	0.21
∑5d Tsoil (0 m), °C	0.18	0.02	−0.03	0.26
∑7d Tsoil (0 m), °C	0.15	0.08	−0.02	0.17
Tsoil (0.75 m), °C	−0.03	0.18	0.47	**0.56**
∑3d Tsoil (0.75 m), °C	0.01	0.23	0.49	**0.57**
∑5d Tsoil (0.75 m), °C	0.00	0.22	0.48	**0.56**
∑7d Tsoil (0.75 m), °C	−0.04	0.19	0.46	0.53
Delta topset water daily discharge Q, $m^3 \cdot s^{-1}$	0.25	0.05	0.24	0.21

accuracy of ERA5 net radiation was observed to have a root mean square error of 19.0 $W \cdot m^{-2}$ and bias of $^{-}0.26$ $W \cdot m^{-2}$. ERA5 showed the most similar data distribution to ground observation data compared to other net radiation products (Seo et al., 2020). To compare these processes against a larger spatial scale in the Arctic, we identified warming trends for the Lena basin, as well as others of the largest catchments of Siberia (Ob and Yenisey) based on the same ERA5 dataset. The Lena basin experiences warming rates of annual temperature of 0.25 $°C \cdot decade^{-1}$ and 0.36 $°C \cdot decade^{-1}$ of cold-season temperature (November–April) during 1936–2019, which differs a little from the Ob and Yenisei River basins. These trends are significantly slower compared to the Lena Delta (Supplementary 6), which is also warming faster than other Arctic regions. The area north of the Arctic Circle experienced an almost fourfold increase in temperature (0.73 $°C \cdot decade^{-1}$) compared to the rest of the world (0.19 $°C \cdot decade^{-1}$) between 1979 and 2021 (Rantanen et al., 2022). Thus, the Lena Delta can be recognized as the world's "hottest spot" in terms of the hydrological consequences of climate change.

The variations in river streamflow, sediment load, and nutrient input to the Lena Delta reflect the impact of the catchment conditions, anthropogenic activities and climate change. However, compared to the climatic trends, there is a significant difference between observed changes at the Kyusyur and Khabarov gauging stations compared with fluctuations in the runoff of the main tributaries in the Lena watershed. The variability of water flow by 43 % was associated with the runoff increase in the upper catchment area by the Tabaga gauging station on the Lena River; 31 % was accounted for by the Aldan River; 20 % was provided with the Vilyui River (Supplementary 3); 6 % is the remaining lateral inflow and channel water balance inconsistencies. The 41 % growth in W_a is provided by an increase in the water content of snowmelt flood (May–July), 29 and 30 % due to the summer–autumn (August–October) and winter low-flow periods. Moreover, the main reasons for the increasing winter runoff and violation of the uniformity of its series are almost equally attributable between natural factors and the impact of the Vilyui reservoir (Berezovskaya et al., 2005; Magritskii, 2008): the operation of the Vilyui reservoir provided additional runoff in winter of ~700 $m^3 \cdot s^{-1}$. The maximum snowmelt flood discharges increased slightly from 134 000 to 138 000 $m^3 \cdot s^{-1}$. The peak of the flood was found to come on average 4 days earlier.

The observed patterns of long-term changes in sediment transport at the top of the Lena Delta compared to other rivers of the Lena basin are even more significant. For example, at the Tabaga gauging station (middle reach of the Lena, ~1800 km upstream), an increase in W_R has been detected only since 2006 (Supplementary 7). The main sources of sediments are the Olekma and Chara rivers, since sediment runoff has decreased on the upper Lena. A decreasing trend was detected in the Aldan basin and its tributaries and explained by the reduction in mining activities in the area. The W_R fluctuations have been similar to those in the lower reaches of the Vilyui and Lena rivers since the late 1980s, but the increase in the Vilyui sediment runoff is limited by the Vilyui reservoir (Magritsky et al., 2022). The growth and time period recorded at the gauging station over the Lena River Delta were the same as those recorded for Kyusyur. Suspended sediment concentration and sediment flow increased in the Lena downstream due to processes in the middle stream of the Lena River (especially in the Olekma basin), and activation of mechanical and ice-rich bank thermal-erosion in the lower reaches of the Vilyui and Lena rivers.

River flow changes across the northern region of the largest rivers are more heterogeneous. Compared to other large polar rivers, the changes observed in the Lena River hydrological regime have several common features – an increase in air temperature and precipitation have led to intensification of the water cycle (Koutsoyiannis, 2020). Results showed that precipitation fluctuations contributed to most of the runoff variations. We compared the data presented herein with water discharges on the large rivers of the Asian part of Russia, such as Salekhard (Ob River, 1930–2020), Igarka (Yenisey River, 1932–2020), Srednekolymsk (Kolyma River, 1927–2020), Tabaga (Lena River, 1927–2020), Verkhoyansky Perevoz (Aldan River, 1935–2020) and Khatyryk-Homo (Vilyui River, 1935–2020) (Supplementary 3). Thus, total runoff from the Eurasian Arctic basin from 1984 to 2018 increased by 0.22 % and 0.24 % per year. River discharge has substantially decreased in the upper Yenisey but increased in the central region of the Lena basin (Feng et al., 2021).

As for the POC and DOC changes, our results indicate that carbon input to the delta is explained by streamflow and sediment concentration. The observed trend in POC and DOC (Fig. 8) is not representative for the long-term hydroclimatic signal, given that the measurements were taken under different flow conditions and thus represent seasonality. Eqs. (9) and (10) show that the increase in average Lena River water discharges from 16 489 $m^3 \cdot s^{-1}$ or 520 km^3 (before 1988) to 18 296 $m^3 \cdot s^{-1}$ or 577 km^3 (during 1988–2020) discussed above, lead to 10% POC increase (e.g., from 0.89 to 0.95 $mg \cdot L^{-1}$, assuming SSC change from 43 to 46 $mg \cdot L^{-1}$). Similar strong seasonal variations in POC concentrations were previously found for six major Arctic rivers (Yenisey, Lena, Ob, Mackenzie, Yukon, Kolyma) (McClelland et al., 2016a). The discharge-concentration relationships observed here are markedly more evident than those reported for the Yenisey, Mackenzie, Yukon, and Ob. This can be explained by the particularly high proportion of yedoma deposits within its drainage area (Strauss et al., 2021), which contribute to riverine POC fluxes through thermokarst activity and bank erosion (Chalov et al., 2022).

4.2. Factors influencing sediment load in the Lena River delta

The sediment regime observed here differs from that of many river deltas of the world. Deltas of the world's rivers are generally associated

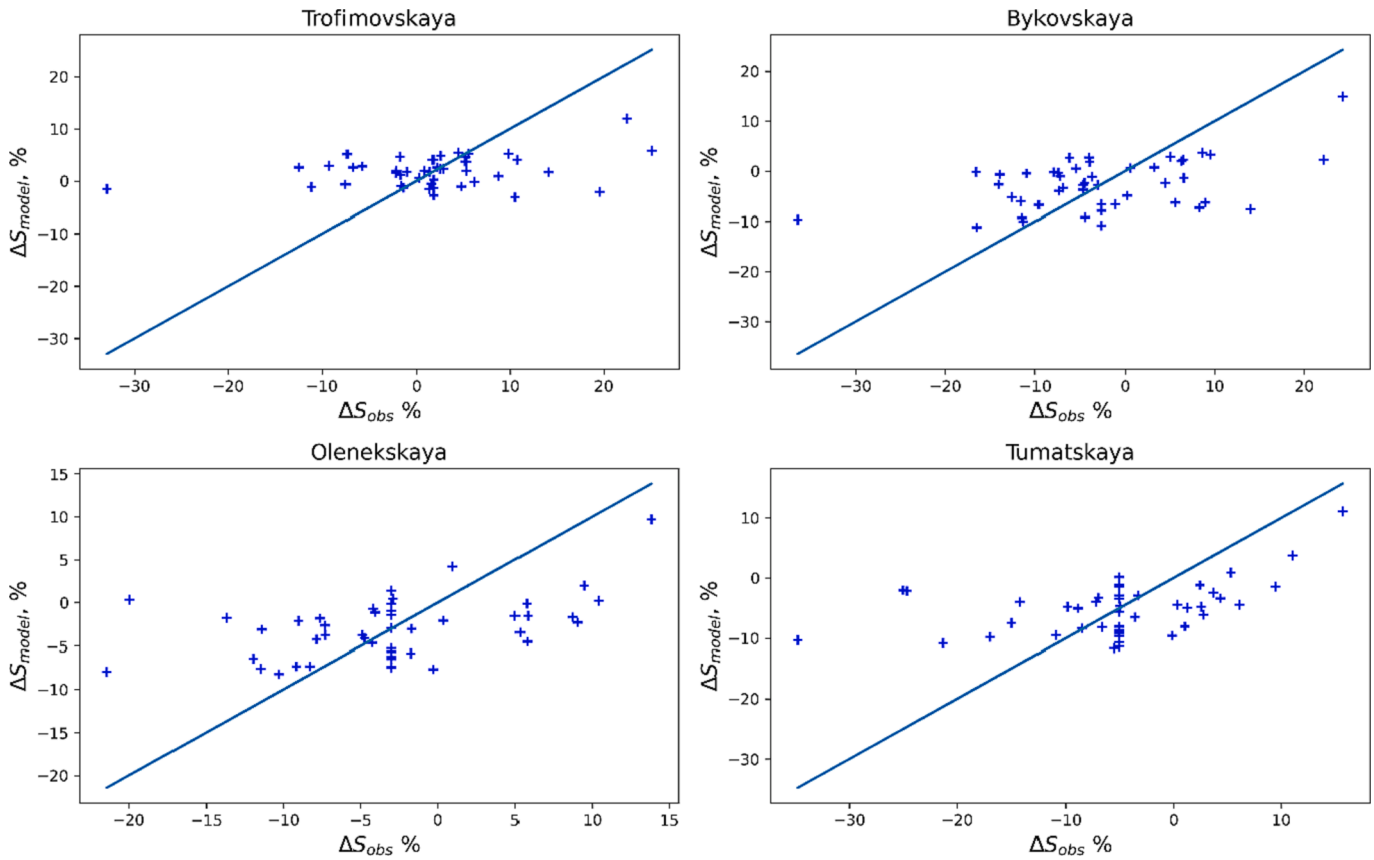

Fig. 7. Relationship between observed daily sediment load change (ΔS_{obs}) and calculated (ΔS_{model}) based on air temperature and wind speed data. Blue line denotes $\Delta S_{obs} = \Delta S_{model}$ relation.

Table 3
Correlation ratios between daily POC and DOC concentrations measured at Kyusyur gauging station.

	Q	SSC	POC	DOC
Q	1.00			
SSC	0.69	1.00		
POC	0.82	0.93	1.00	
DOC	0.74	0.42	0.57	1.00

Note: POC and DOC are for the Zhigansk station; SSC and Q are for the Kyusyur station. Q data are corrected for the distance between Zhigansk and Kyusyur.

with a decrease in hydraulic gradient and a reduction in sediment transport conditions, forming (re)depositional environments that are often characterized by mudflats and tidal wetlands (Fryirs et al., 2007). Increased water discharges and elevation levels favor hydraulic connectivity between the main channels and adjacent deltaic environments (Heiler et al., 1995; Pietroń et al., 2018), enhancing sediment conveyance from the main channel to the deltaic plain and inducing sediment storage. Flooding dynamics govern the net accumulation rates over delta plain across the Mekong River delta, which stores on average 28 % of the incoming sediment load (Binh et al., 2020; Szczuciński et al., 2013). The Selenga River delta, which is the largest tributary of Lake Baikal, can store as much as 34 % of the incoming suspended sediment load (and 67 % of the total sediment load) during high-flow conditions (Chalov et al., 2017; Dong et al., 2016), likely due to an increase in connectivity between channels and floodplain water bodies. These studies also suggested the ability of the delta to store sediment due to evolution of the vegetation cover and seasonal fluctuation of the recipient waterbody's water levels, which can generate backwater effects (Pietroń et al., 2018;

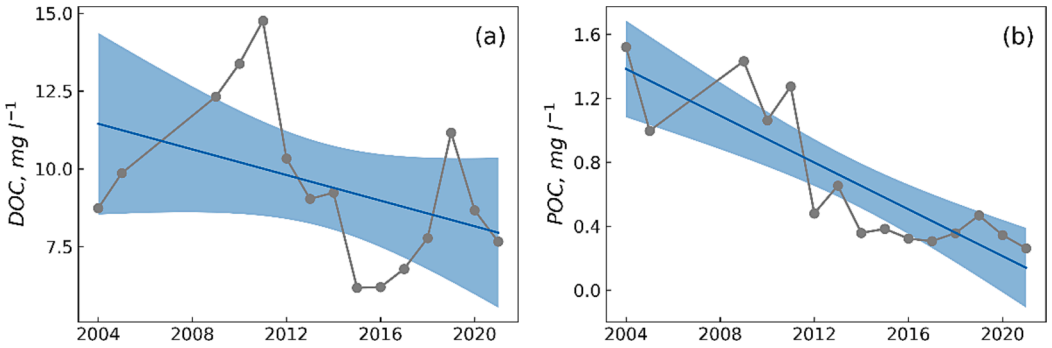

Fig. 8. Long-term changes in (a) DOC and (b) POC concentrations to the Lena Delta. The overall linear trend for 2004–21 is shown (blue line), with its 95% confidence interval; gray point is mean annual value.

Shinkareva et al., 2019).

In the Lena Delta, the observed rise in air temperature and streamflow input coincides with remobilization of sediments. Our study suggests that streamflow conditions, the duration of freezing, frozen, thawing, and unfrozen periods, and riverbank susceptibility to erosion contribute to sediment load through thermokarst activity and bank erosion across the Lena Delta. Increases in streamflow and air temperature impact the rates of freezing/thawing and fluvial bank erosion (Peng et al., 2010). The spring flood inundates the low floodplains and the shallow gullies that are usually dry in the other months (Pertiwi et al., 2021), which do not have extended space to accommodate sediments. The conditions in the Lena River Delta are related to the absence of macrophytes and, thus, this biofiltering effect usually important in the deltas located in the moderate and tropical climate is also negligible (Shinkareva et al., 2019).

The complex interaction between various drivers hampers the establishment of significant relationships between particular factors controlling sediment transport (Table 2). For example, very contrasting sediment transport patterns are observed under the same streamflow conditions. In some cases, the impact of increased water discharges is evident: the highest Lena River water discharge in our satellite imagery dataset (10 June 2018, Q = 78 100 $m^3 \cdot s^{-1}$) coincides with the highest rates of downstream sediment increasing along delta distributaries (ΔS = 67.1 % along Bykovskaya, 41.5 % along Trofimovskaya, 41.5 % along Tumatskaya and 73.9 % along Olenekskaya) (Supplementary 8 – a). It is important to note that the satellite image analysis is limited by the conditions of ice-free flow (from June to September) and the whole dataset generally contains 47 situations (images). This flux within the ice-free period accounts for up to 95 % of the annual sediment yield.

The significant correlations between sediment transport conditions and air and soil temperatures (Table 2) are another example of the impact of hydroclimatic changes on the sediment transport conditions over the delta. As stated by Fedorova et al. (2015), the annual cutoff of riverbank edges during high water produces an unmeasured quantity of suspended and bottom sediments. Additional sediments are washed into the river by thermal erosion and thermal denudation of permafrost banks, which actively thaw under maximal temperatures. These patterns are recorded throughout SSC maps (Supplementary 8 – b and c), which demonstrate a significant increase (ΔS >10 %) in sediment concentration along the delta. In particular, the soil temperature at the depth of 0.75 m strongly correlated with relative increases in suspended sediment transport. An increase in temperature leads to the activation of the destruction of the riverbanks, which are composed of an ice complex. According to Rachold et al. (2000), sediment volume contribution through thermal erosion processes is almost 2.5 times as great as the fluvial sediment fluxes. Landsat images processing show significant planform change across the Lena Delta. The maximum rate of erosion is observed in the Trofimovskaya branch, whose riverbank sediments mainly consist of yedoma – fine-grained materials rich in organics and ice. This segment of the delta is also noted in our study as the most efficient in sediment mobilization (average ΔS=+8.94 %).

A positive relationship between SSC change (ΔS) and precipitation was observed for the Olenekskaya branch. The effect of precipitation on the SSC increase is associated with the local inflow of turbid waters flowing down from the Verkhoyansky ridges on the left bank. Wind speed rise is associated with higher SSC in the Bykovskaya and Tumatskaya channels. Wind is an important form of natural disturbance that drives SSC by disturbing bed material or blowing of braid bars. Additional impacts on the sediment budget in the Arctic deltas are related to coastal upwelling events, which regularly increase sea-surface turbidity in certain areas adjacent to the Lena Delta in the Laptev Sea and the Kolyma Deltas in the East-Siberian Sea (Osadchiev et al., 2020). These events are formed under strong easterly and south-easterly wind forcing and are estimated to occur during up to 10 % – 30 % of ice-free periods. Combined with intensive coastal erosion (Shakhova et al., 2007), these upwelling events increase sediment concentrations in the most downstream parts of the Lena distributaries.

Stream temperature is another possible factor influencing the frozen banks' thermal erosion and thus increasing sediment transport across the delta (Costard et al., 2007). The water temperature in June, July–August, and September increased by 1.1, 0.6 and 0.05 °C (as shown for the Kyusyur station, see 3.2) which can impact the sediment regime in a long-term perspective. As shown by Gautier et al. (2021), for the lower Lena, water temperatures affect the subsequent thawing of ice, reducing the islands' strength and increasing erosion efficiency. Additionally, thermal effect of global warming on sediment mobilization was proved by experimental studies (Ramalingam and Chandra, 2020), which show that a rise in water temperature causes decreases in both settling flux and degree of deposition.

5. Conclusions

This study analyzed changes in air and soil temperature, precipitation, and wind speed across the Lena River Delta and their relations with streamflow, sediment load, and carbon fluxes. Along with the substantial increase in air temperatures, there have also been increases in streamflow, sediment, and heat flux input to the delta over recent decades. While the flow partitioning between major distributaries remains constant, the sediment transport conditions have changed significantly. The impact of rising air and soil temperatures on bank degradation and the impact of wind on bottom sediments are considered to be the main drivers of suspended sediment dynamics.

The observed hydroclimatic and sediment transport changes over the Lena Delta are higher than those of the Lena catchment and other major polar rivers. These results imply that the Lena Delta should be recognized as the greatest global hot spot in terms of hydrological consequences of climate change. The significant increase in water and sediment discharge entering the delta and the hydroclimatic impacts on sedimentation patterns across the delta reflect the ongoing climate-driven evolution of the system.

This study provides quantitative results of climate–water–sediment–nutrient variations in the largest polar delta. The main novelty of this study is the integrated picture it provides of long-term changes from a regional perspective. The specific regime of the Lena Delta shines light on a variety of ecological impacts (e.g., production of plant biomass) and biogeochemical impacts (e.g., microbial degradation) controlled by variations in sediment and dissolved (DOC) and particulate organic carbon (POC). The study's results contain valuable information that can be used in developing strategies to cope with and mitigate the dramatic effects of sediment mobilization due to recent global warming in the Arctic, and to detect and predict possible coastal ecosystem degradation in future.

CRediT authorship contribution statement

Sergey Chalov: Conceptualization, Writing – original draft, Investigation. **Kristina Prokopeva:** Investigation, Methodology. **Dmitry Magritsky:** Methodology, Investigation. **Vadim Grigoriev:** Methodology, Validation. **Evgeniya Fingert:** Data curation, Formal analysis. **Michal Habel:** Conceptualization. **Bennet Juhls:** Methodology, Writing – review & editing. **Anne Morgenstern:** Writing – review & editing. **Pier Paul Overduin:** Writing – review & editing. **Nikolay Kasimov:** .

Declaration of Competing Interest

The authors declare that they have no known competing financial interests or personal relationships that could have appeared to influence the work reported in this paper.

Data availability

Data will be made available on request.

Acknowledgements

Fieldworks, study concept and numerical simulations are done within the implementation of Russian Science Foundation project 21-17-00181. Additionally, the remote-sensing processing has been supported by the Kazan Federal University Strategic Academic Leadership Program ("PRIORITY-2030"). The authors greatly acknowledge the support of Samoylov Island Research Station. The authors also acknowledge Mr. Tim Brombley for language editing.

Appendix A. Supplementary data

Supplementary data to this article can be found online at https://doi.org/10.1016/j.ecolind.2023.111252.

References

Berezovskaya, S., Yang, D., Hinzman, L., 2005. Long-term annual water balance analysis of the Lena River. Glob. Planet. Change. https://doi.org/10.1016/j.gloplacha.2004.12.006.

Binh, D.V., Kantoush, S., Sumi, T., 2020. Changes to long-term discharge and sediment loads in the Vietnamese Mekong Delta caused by upstream dams. Geomorphology. https://doi.org/10.1016/j.geomorph.2019.107011.

Boike, J., Kattenstroth, B., Abramova, K., Bornemann, N., Chetverova, A., Fedorova, I., Fröb, K., Grigoriev, M., Grüber, M., Kutzbach, L., Langer, M., Minke, M., Muster, S., Piel, K., Pfeiffer, E.M., Stoof, G., Westermann, S., Wischnewski, K., Wille, C., Hubberten, H.W., 2013. Baseline characteristics of climate, permafrost and land cover from a new permafrost observatory in the Lena River Delta, Siberia (1998–2011). Biogeosciences. https://doi.org/10.5194/bg-10-2105-2013.

Boike, J., Nitzbon, J., Anders, K., Grigoriev, M., Bolshiyanov, D., Langer, M., Lange, S., Bornemann, N., Morgenstern, A., Schreiber, P., Wille, C., Chadburn, S., Gouttevin, I., Burke, E., Kutzbach, L., 2019. A 16-year record (2002–2017) of permafrost, active-layer, and meteorological conditions at the Samoylov Island Arctic permafrost research site, Lena River delta, northern Siberia: an opportunity to validate remote-sensing data and land surface, snow, and. Earth Syst. Sci. Data 11, 261–299. https://doi.org/10.5194/essd-11-261-2019.

Bolshiyanov, D.Y., Makarov, A.S., Schneider, V., Stoof, G., 2013. Origin and development of the Lena River Delta. AARI, St. Petersburg.

Chalov, S.R., Moreido, V.M., Prokopeva, K.N., Efimov, V.A., 2022. Implications of yedoma bank outcrops on the arctic rivers sediment runoff. Hydrosphere. Hazard Process. Phenom. 4, 165–182. https://doi.org/10.34753/HS.2022.4.2.165.

Chalov, S., Prokopeva, K., 2022. Sedimentation and Erosion Patterns of the Lena River Anabranching Channel. Water 14, 3845. https://doi.org/10.3390/w14233845.

Chalov, S., Thorslund, J., Kasimov, N., Aybullatov, D., Ilyicheva, E., Karthe, D., Kositsky, A., Lychagin, M., Nittrouer, J., Pavlov, M., Pietron, J., Shinkareva, G., Tarasov, M., Garmaev, E., Akhtman, Y., Jarsjö, J., 2017. The Selenga River delta: a geochemical barrier protecting Lake Baikal waters. Reg. Environ. Chang. 17, 2039–2053. https://doi.org/10.1007/s10113-016-0996-1.

Chalov, S., Prokopeva, K., Habel, M., 2021. North to South Variations in the Suspended Sediment Transport Budget within Large Siberian River Deltas Revealed by Remote Sensing Data. Remote Sens. 13, 4549. https://doi.org/10.3390/rs13224549.

Chalov, S.R., Prokopeva, K.N., 2021. Assessment of Suspended Sediment Budget of the Lena River Delta Based on the Remote Sensing Dataset. Izv. Atmos. Ocean. Phys. 57, 1051–1060. https://doi.org/10.1134/S0001433821090450.

Costard, F., Dupeyrat, L., Gautier, E., Carey-Gailhardis, E., 2003. Fluvial thermal erosion investigations along a rapidly eroding riverbank: Application to the Lena River (Central Siberia). arth Surf. Process. Landforms 1349–1359.

Costard, F., Gautier, E., Brunstein, D., Hammadi, J., Fedorov, A., Yang, D., Dupeyrat, L., 2007. Impact of the global warming on the fluvial thermal erosion over the Lena River in Central Siberia. Geophys. Res. Lett. 34 https://doi.org/10.1029/2007GL030212.

Demchev, D.M., Kulakov, M.Y., Makshtas, A.P., Makhotina, I.A., Fil'chuk, K.V., Frolov, I. E., 2020. Verification of ERA-Interim and ERA5 Reanalyses Data on Surface Air Temperature in the Arctic. Russ. Meteorol. Hydrol. 45, 771–777. https://doi.org/10.3103/S1068373920110035.

Dentener, F.J., Easterling, D.R., Uk, Richard Allan, Uk, Robert Allan, Cooper, O., Canada, F., Uk, J.K., Uk, E.K., Germany, S.K., Uk, C.M., Morice, C., 2013. IPCC Climate Change 2013: The Physical Science Basis. Chapter 2: Observations: Atmosphere and Surface. Clim. Chang. 2013 Phys. Sci. Basis Work. Gr. I Contrib. to Fifth Assess. Rep. Intergov. Panel Clim. Chang. 9781107057.

Dong, T.Y., Nittrouer, J.A., Il'icheva, E., Pavlov, M., McElroy, B., Czapiga, M.J., Ma, H., Parker, G., 2016. Controls on gravel termination in seven distributary channels of the Selenga River Delta, Baikal Rift basin, Russia. Geol. Soc. Am. Bull. 128, 1297–1312. https://doi.org/10.1130/B31427.1.

Fedorova, I., Chetverova, A., Bolshiyanov, D., Makarov, A., Boike, J., Heim, B., Morgenstern, A., Overduin, P.P., Wegner, C., Kashina, V., Eulenburg, A., Dobrotina, E., Sidorina, I., 2015. Lena Delta hydrology and geochemistry: Long-term hydrological data and recent field observations. Biogeosciences. https://doi.org/10.5194/bg-12-345-2015.

Feng, D., Gleason, C.J., Lin, P., Yang, X., Pan, M., Ishitsuka, Y., 2021. Recent changes to Arctic river discharge. Nat. Commun. 2021 121 12, 1–9. https://doi.org/10.1038/s41467-021-27228-1.

Fryirs, K.A., Brierley, G.J., Preston, N.J., Kasai, M., 2007. Buffers, barriers and blankets: The (dis)connectivity of catchment-scale sediment cascades. Catena. https://doi.org/10.1016/j.catena.2006.07.007.

Gautier, E., Dépret, T., Cavero, J., Costard, F., Virmoux, C., Fedorov, A., Konstantinov, P., Jammet, M., Brunstein, D., 2021. Fifty-year dynamics of the Lena River islands (Russia): Spatio-temporal pattern of large periglacial anabranching river and influence of climate change. Sci. Total Environ. 783 https://doi.org/10.1016/j.scitotenv.2021.147020.

Heiler, G., Hein, T., Schiemer, F., Bornette, G., 1995. Hydrological connectivity and flood pulses as the central aspects for the integrity of a river-floodplain system. Regul. Rivers Res. Manag. https://doi.org/10.1002/rrr.3450110309.

Holmes, R.M., McClelland, J.W., Peterson, B.J., Tank, S.E., Bulygina, E., Eglinton, T.I., Gordeev, V.V., Gurtovaya, T.Y., Raymond, P.A., Repeta, D.J., Staples, R., Striegl, R. G., Zhulidov, A.V., Zimov, S.A., 2012. Seasonal and Annual Fluxes of Nutrients and Organic Matter from Large Rivers to the Arctic Ocean and Surrounding Seas. Estuaries and Coasts. https://doi.org/10.1007/s12237-011-9386-6.

Ivanov, V.V., Piskun, A.A., Korabel, R.A., 1983. Distribution of Runoff through the Main Channels of the Lena River Delta (In Russian). Tr. AANI (proceedings AARI) 378, 59–71.

Juhls, B., Stedmon, C.A., Morgenstern, A., Meyer, H., Hölemann, J., Heim, B., Povazhnyi, V., Overduin, P.P., 2020. Identifying Drivers of Seasonality in Lena River Biogeochemistry and Dissolved Organic Matter Fluxes. Front. Environ. Sci. 8 https://doi.org/10.3389/fenvs.2020.00053.

Koutsoyiannis, D., 2020. Revisiting the global hydrological cycle: Is it intensifying? Hydrol. Earth Syst. Sci. 24, 3899–3932. https://doi.org/10.5194/HESS-24-3899-2020.

Magritskii, D.V., 2008. Anthropogenic Impact on the Runoff of Russian Rivers Emptying into the Arctic Ocean. Water Res. 35, 1–14.

Magritsky, D.V., 2015. Factors and patterns of long-term changes in water flow, suspended sediments and heat of the Lower Lena and Vilyui. Vestn. Moscow. Un-Ta. Ser. Geogr. 5, 85–89.

Magritsky, D.V., Alexeevsky, N.I., Aybulatov, D.N., Fofonova, V.V., Gorelkin, A., 2018. Features and evaluations of spatial and temporal changes of water runoff, sediment yield and heat flux in the Lena River delta. Polarforschung 87, 89–110. https://doi.org/10.2312/polarforschung.87.2.89.

Magritsky, D., Moreido, V., Prokopeva, K., 2022. CHANGES IN THE RUNOFF OF SUSPENDED SEDIMENTS OF THE VILYUY RIVER BY THE CASCADE OF RESERVOIRS. HYDROSPHERE. HAZARD Process. Phenom. 4, 68-92 (In Russian; abstract in English). https://doi.org/10.34753/HS.2022.4.1.68.

Mallakpour, I., Villarini, G., 2016. A simulation study to examine the sensitivity of the Pettitt test to detect abrupt changes in mean. Hydrol. Sci. J. 61, 245–254. https://doi.org/10.1080/02626667.2015.1008482.

Mann, H.B., Whitney, D.R., 1947. On a test of whether one of two random variables is stochastically larger than the other. Ann. Math. Stat. 18, 50–60. https://doi.org/10.1214/aoms/1177730491.

Matsuoka, A., Babin, M., Vonk, J.E., 2022. Decadal trends in the release of terrigenous organic carbon to the Mackenzie Delta (Canadian Arctic) using satellite ocean color data (1998–2019). Remote Sens. Environ. 283 https://doi.org/10.1016/j.rse.2022.113322.

McClelland, J.W., Holmes, R.M., Peterson, B.J., Raymond, P.A., Striegl, R.G., Zhulidov, A.V., Zimov, S.A., Zimov, N., Tank, S.E., Spencer, R.G.M., Staples, R., Gurtovaya, T.Y., Griffin, C.G., 2016a. Particulate organic carbon and nitrogen export from major Arctic rivers. Global Biogeochem. Cycles 30, 629–643. https://doi.org/10.1002/2015GB005351.

McClelland, J.W., Holmes, R.M., Peterson, B.J., Raymond, P.A., Striegl, R.G., Zhulidov, A.V., Zimov, S.A., Zimov, N., Tank, S.E., Spencer, R.G.M., Staples, R., Gurtovaya, T.Y., Griffin, C.G., 2016b. Particulate organic carbon and nitrogen export from major Arctic rivers. Global Biogeochem. Cycles. https://doi.org/10.1002/2015GB005351.

Morehead, M.D., Syvitski, J.P., Hutton, E.W.H., Peckham, S.D., 2003. Modeling the temporal variability in the flux of sediment from ungauged river basins. Glob. Planet. Change 39. https://doi.org/10.1016/S0921-8181(03)00019-5.

Muñoz-Sabater, J., 2019. ERA5-Land monthly averaged data from 1981 to present. Copernicus Climate Change Service (C3S) Climate Data Store. Clim. Data Store.

Naghettini, M., 2016. Fundamentals of statistical hydrology. Fundamentals of Statistical Hydrology. https://doi.org/10.1007/978-3-319-43561-9.

Osadchiev, A., Silvestrova, K., Myslenkov, S., 2020. Wind-Driven Coastal Upwelling near Large River Deltas in the Laptev and East-Siberian Seas. Remote Sens. 12, 844. https://doi.org/10.3390/rs12050844.

Pavelsky, T.M., Smith, L.C., 2009. Remote sensing of suspended sediment concentration, flow velocity, and lake recharge in the Peace-Athabasca Delta. Canada. Water Resour. Res. 45 https://doi.org/10.1029/2008WR007424.

Peng, J., Chen, S., Dong, P., 2010. Temporal variation of sediment load in the Yellow River basin, China, and its impacts on the lower reaches and the river delta. Catena 83, 135–147. https://doi.org/10.1016/j.catena.2010.08.006.

Pertiwi, A.P., Roth, A., Schaffhauser, T., Bhola, P.K., Reuß, F., Stettner, S., Kuenzer, C., Disse, M., 2021. Monitoring the spring flood in lena delta with hydrodynamic modeling based on sar satellite products. Remote Sens. 13 https://doi.org/10.3390/rs13224695.

Pettitt, A.N., 1979. A Non-Parametric Approach to the Change-Point Problem. Appl. Stat. https://doi.org/10.2307/2346729.

Pietroń, J., Nittrouer, J.A., Chalov, S.R., Dong, T.Y., Kasimov, N., Shinkareva, G., Jarsjö, J., 2018. Sedimentation patterns in the Selenga River delta under changing

hydroclimatic conditions. Hydrol. Process. 32, 278–292. https://doi.org/10.1002/hyp.11414.

Rachold, V., Grigoriev, M., Are, F., Solomon, S., Reimnitz, E., Kassens, H., Antonow, M., 2000. Coastal erosion vs riverine sediment dischardge in the Arctic Shelf seas. Int. J. Earth Sci 450–460.

Ramalingam, S., Chandra, V., 2020. Effect of Water Temperature on Suspended Sediment Concentration and Particle Size in Ionized Water. Iran. J. Sci. Technol. - Trans. Civ. Eng. 44 https://doi.org/10.1007/s40996-020-00460-3.

Rantanen, M., Karpechko, A.Y., Lipponen, A., Nordling, K., Hyvärinen, O., Ruosteenoja, K., Vihma, T., Laaksonen, A., 2022. The Arctic has warmed nearly four times faster than the globe since 1979. Commun. Earth Environ. 3, 1–10. https://doi.org/10.1038/s43247-022-00498-3.

Schneider, J., Grosse, G., Wagner, D., 2009. Land cover classification of tundra environments in the Arctic Lena Delta based on Landsat 7 ETM+ data and its application for upscaling of methane emissions. Remote Sens. Environ. https://doi.org/10.1016/j.rse.2008.10.013.

Seo, M., Kim, H.C., Lee, K.S., Seong, N.H., Lee, E., Kim, J., Han, K.S., 2020. Characteristics of the Reanalysis and Satellite-Based Surface Net Radiation Data in the Arctic. J. Sensors 2020. https://doi.org/10.1155/2020/8825870.

Shakhova, N., Semiletov, I., Bel'cheva, N., 2007. The great Siberian rivers as a source of methane on the Russian Arctic shelf. Dokl. Earth Sci. 415, 734–736. https://doi.org/10.1134/S1028334X07050169.

Sherjah, P.Y., Sajikumar, N., Nowshaja, P.T., 2023. Quality monitoring of inland water bodies using Google Earth Engine. J. Hydroinformatics 25, 432–450. https://doi.org/10.2166/hydro.2023.137.

Shiklomanov, A.I., Yakovleva, T.I., Lammers, R.B., Karasev, I.P., Vörösmarty, C.J., Linder, E., 2006. Cold region river discharge uncertainty-estimates from large Russian rivers. J. Hydrol. https://doi.org/10.1016/j.jhydrol.2005.10.037.

Shinkareva, G.L., Lychagin, M.Y., Tarasov, M.K., Pietroń, J., Chichaeva, M.A., Chalov, S. R., 2019. Biogeochemical specialization of macrophytes and their role as a biofilter in the Selenga delta. Geogr. Environ. Sustain. 12, 240–263. https://doi.org/10.24057/2071-9388-2019-103.

Strauss, J., Laboor, S., Schirrmeister, L., Fedorov, A.N., Fortier, D., Froese, D., Fuchs, M., Günther, F., Grigoriev, M., Harden, J., Hugelius, G., Jongejans, L.L., Kanevskiy, M., Kholodov, A., Kunitsky, V., Kraev, G., Lozhkin, A., Rivkina, E., Shur, Y., Siegert, C., Spektor, V., Streletskaya, I., Ulrich, M., Vartanyan, S., Veremeeva, A., Anthony, K. W., Wetterich, S., Zimov, N., Grosse, G., 2021. Circum-Arctic Map of the Yedoma Permafrost Domain. Front. Earth Sci. 9 https://doi.org/10.3389/feart.2021.758360.

Syvitski, J.P.M., Vörösmarty, C.J., Kettner, A.J., Green, P., 2005. Impact of humans on the flux of terrestrial sediment to the global coastal ocean. Science 80 (308), 376–380. https://doi.org/10.1126/science.1109454.

Szczuciński, W., Jagodziński, R., Hanebuth, T.J.J., Stattegger, K., Wetzel, A., Mitręga, M., Unverricht, D., Van Phach, P., 2013. Modern sedimentation and sediment dispersal pattern on the continental shelf off the Mekong River delta. South China Sea. Glob. Planet. Change 110, 195–213. https://doi.org/10.1016/j.gloplacha.2013.08.019.

Vihma, T., Uotila, P., Sandven, S., Pozdnyakov, D., Makshtas, A., Pelyasov, A., Pirazzini, R., Danielsen, F., Chalov, S., Lappalainen, H.K., Ivanov, V., Frolov, I., Albin, A., Cheng, B., Dobrolyubov, S., Arkhipkin, V., Myslenkov, S., Petäjä, T., Kulmala, M., 2019. Towards an advanced observation system for the marine Arctic in the framework of the Pan-Eurasian Experiment (PEEX). Atmos. Chem. Phys. 19, 1941–1970. https://doi.org/10.5194/acp-19-1941-2019.

Wild, B., Andersson, A., Bröder, L., Vonk, J., Hugelius, G., McClelland, J.W., Song, W., Raymond, P.A., Gustafsson, Ö., 2019. Rivers across the Siberian Arctic unearth the patterns of carbon release from thawing permafrost. Proc. Natl. Acad. Sci. 116, 10280–10285. https://doi.org/10.1073/pnas.1811797116.

Yin, F., Lewis, P.E., Gómez-Dans, J.L., 2022. Bayesian atmospheric correction over land: Sentinel-2/MSI and Landsat 8/OLI. Geosci. Model Dev. 15, 7933–7976. https://doi.org/10.5194/gmd-15-7933-2022.

Yue, S., Pilon, P., Cavadias, G., 2002. Power of the Mann-Kendall and Spearman's rho tests for detecting monotonic trends in hydrological series. J. Hydrol. 259, 254–271.